Wetzel, R., Perry, L. J., Estell, D. A., Lin, N., Levine, H. L., Slinker, B., Fields, F., Ross, M. J., & Shively, J. (1981) *J. Interferon Res. 1*, 381–390.
Wetzel, R., Levine, H. L., Estell, D. A., Shire, S., Finer-Moore, L., Stroud, R. M., & Bewley, T. A. (1982) *UCLA Symp. Mol. Cell. Biol. 25*, 365–376.
Wetzel, R., Johnston, P. D., & Czarniecki, C. (1983) in *Biology of the Interferon System* (Schellekens, H., et al., Eds.) pp 101–112, Elsevier, New York.
Yonehara, S., Yonehara-Takahashi, M., Ishu, A., & Nagata, S. (1983) *J. Biol. Chem. 258*, 9046–9049.
Zoon, K. C., & Wetzel, R. (1983) in *Handbook of Experimental Pharmacology* (Came, P. E., & Carter, W. A., Eds.) pp 79–100, Springer-Verlag, New York.

Macrophage Recognition of Immune Complexes: Development and Application of Novel Cell Surface Labeling Procedures†

Howard R. Petty* and William Dereski
Department of Biological Sciences, Wayne State University, Detroit, Michigan 48202
Received January 24, 1985

ABSTRACT: A fluorescein- and lactoperoxidase-conjugated ferritin–anti-ferritin immune complex has been prepared for cell surface labeling experiments on immune recognition and effector function. Lactoperoxidase (LPO) has been covalently coupled to affinity-purified anti-ferritin antibodies with *p*-benzoquinone by a modified version of the method of Ternynck and Avrameas [Ternynck, T., & Avrameas, S. (1976) *Ann. Immunol. (Paris) 127C*, 197]. The conjugate is a heterodimer of M_r 230 000 with linkages to either or both of the heavy and light chains of the antibody, as judged by two-dimensional sodium dodecyl sulfate–polyacrylamide gel electrophoresis (SDS–PAGE) in the absence and presence of 2-mercaptoethanol. The conjugate retains antibody-binding activity as measured by a quantitative precipitin assay. When incorporated into immune complexes, the modified antibody also retains Fc receptor recognition ability as determined by erythrocyte–antibody rosette inhibition assays. Electron microscopy demonstrated that the antigen, ferritin, was monodisperse with complete apoprotein sheaths surrounding the core. Ferritin–anti-ferritin–LPO complexes were formed in 4-fold antigen excess. Complexes were verified by fluorescence and electron microscopy. Immune complexes were masked with "cold" iodine by use of the endogenous LPO activity. The complexes bound to cells at 4 °C as shown by electron microscopy and fluorescence video/intensification microscopy. The LPO delivered to the cell surface in this fashion can be utilized to iodinate the surface with ^{125}I. Under saturation conditions, the labeling with local LPO delivery followed by SDS–PAGE and autoradiography is identical with labeling with free LPO. Labeling has also been conducted under conditions of substrate deficit. In addition, bovine serum albumin has been employed to scavenge I^+, which may diffuse from the local LPO delivery sites. These conditions reveal that, during immune complex recognition, a local polymerization reaction occurs that can be at least partially reversed with 2-mercaptoethanol.

Macrophage cell surface receptors for the Fc domain of the immunoglobulin molecule can mediate immunologic recognition and trigger the internalization of particulate and soluble immune complexes. Studies on the nature of the Fc receptor typically employ erythrocyte–antibody rosetting or radiolabeled ligand binding measurements (Leslie & Alexander, 1980; Zuckerman & Douglas, 1979a,b). Recently, Mellman & Unkeless (1980) have employed a monoclonal anti-Fc receptor antibody to characterize this membrane glycoprotein. The receptor has been shown to function as a ligand-dependent ion channel (Young et al., 1983a,b). This change in membrane potential is likely associated with subsequent metabolic alterations. However, the biochemical events that accompany the triggering of endocytosis are not well characterized. In a recent study we have shown that membrane-impermeable sulfhydryl-blocking reagents inhibit endocytosis, but not binding, of immune complexes at nanomolar concentrations (Dereski & Petty, 1985). This suggests that a cell surface sulfhydryl group is associated with the triggering of endocytosis.

In this paper we describe the properties of model immune complexes that combine the advantages of morphological and biochemical analyses. These complexes (1) can be examined by fluorescence and electron microscopy and (2) provide an antibody-dependent method to deliver lactoperoxidase (LPO) to localized regions of immune recognition at the cell surface for simultaneous labeling with radioactive iodine. The results are relevant to understanding the transmembrane signaling required for endocytosis.

Materials and Methods

Cell Culture. The murine RAW264 macrophage cell line and the human U937 monocytic cell line were employed in these studies. Their origins and properties have been previously described (Raschke et al., 1978; Sundstrom & Nilsson, 1976; Petty et al., 1980a). The U937 cell line was obtained from the American Type Culture Collection (Bethesda, MD). The RAW264 cell line was grown as adherent cells. The U937

† This work was supported by NIH Grant AI-19075.

0006-2960/85/0424-4141$01.50/0

cells were grown in suspension culture. Both cell lines were grown in RPMI 1640 medium (Gibco, Grand Island, NY) containing 10% fetal calf serum (Calbiochem, San Diego) and 10 μg/mL penicillin–streptomycin (Gibco). The RAW264 macrophages were removed from the tissue culture flasks by incubation for 15–30 min with Hank's balanced salt solution (HBSS) without Ca^{2+} or Mg^{2+} containing 2 mM ethylenediaminetetraacetic acid (EDTA). The cells were then washed twice with the appropriate buffer.

Protein and Iron Determinations. Protein concentrations were routinely determined by the method of Lowry et al. (1951) with bovine serum albumin (BSA) as standard. The iron content of ferritin or ferritin–anti-ferritin complexes was determined by the absorbance at 310 nm according to the method of Lauber (1965); 10 μg/mL ferritin iron is equivalent to an extinction of 0.76. Antibody has a negligible absorbance at this wavelength. For antibody concentrations, the absorbance at 280 nm was used as described (Hudson & Hay, 1980).

Ferritin. Ferritin was routinely chromatographed on Sephacryl G-200 prior to use. Precipitation with $CdSO_4$ and $(NH_4)_2SO_4$ was performed as described (Rifkind et al., 1963) when required, depending upon commercial sources.

Anti-ferritin Antibodies. Rabbit anti-horse ferritin antibody was purchased from Cappel Laboratories (Cochranville, PA). Immunoglobulin G (IgG) was fractionated from the serum by affinity chromatography on protein A–agarose beads using acetate buffer at pH 4.5 for elution. The purified antibody migrated as single band on sodium dodecyl sulfate–polyacrylamide gel electrophoresis (SDS–PAGE).

Conjugation of Antibody with LPO. Purified rabbit anti-horse ferritin antibody was conjugated to LPO with *p*-benzoquinone as described by Ternynck & Avrameas (1976). Benzoquinone is capable of forming 1,4-addition products with thiols and amino groups of proteins (Morrison et al., 1969; Bourguignon, 1979). Antibody (20 mg) at 6.67 mg/mL was dialyzed against phosphate buffer at pH 6.0. *p*-Benzoquinone (Eastman Kodak, Rochester, NY; catalog no. P220) was dissolved in ethanol at 40 mg/mL. An aliquot (0.5 mL) of this was then added to the antibody. The test tube was covered with aluminum foil and incubated for 30 min at room temperature. The solution was then passed through a Sephadex G-25 column (Pharmacia, Piscataway, NJ) with use of normal saline for elution. Unreacted benzoquinone and protein aggregates collected near the top of the column. Activated antibody (molecular weight far above the exclusion point) ran as a pink band in the column and was collected from the effluent. Twenty milligrams of LPO in saline was immediately added to this, followed by one-tenth solution volume of 1 M carbonate–bicarbonate buffer, pH 9.0. After 18 h at room temperature one-tenth solution volume of 1 M lysine (Sigma) at pH 7.5 was added to stop the reaction. The conjugate was dialyzed against phosphate-buffered saline (PBS) and stored in a refrigerator in the presence of 0.01% sodium azide.

Purification of Antibody–LPO Conjugates. Conjugates were purified by Sephacryl S-200 and Sephacryl S-400 column chromatography (Pharmacia). Free LPO and antibody are separated from conjugates by S-200 chromatography. The conjugates are a somewhat heterogeneous collection of oligomers. A primary antibody–LPO dimer can be obtained from S-400 chromatography. In all cases PBS + 0.01% sodium azide was employed as the buffer. In Figure 1 we show a schematic diagram of our experimental procedures.

Conjugation of Ferritin with FITC. Purified ferritin was conjugated with fluorescein isothiocyanate (FITC) (Sigma)

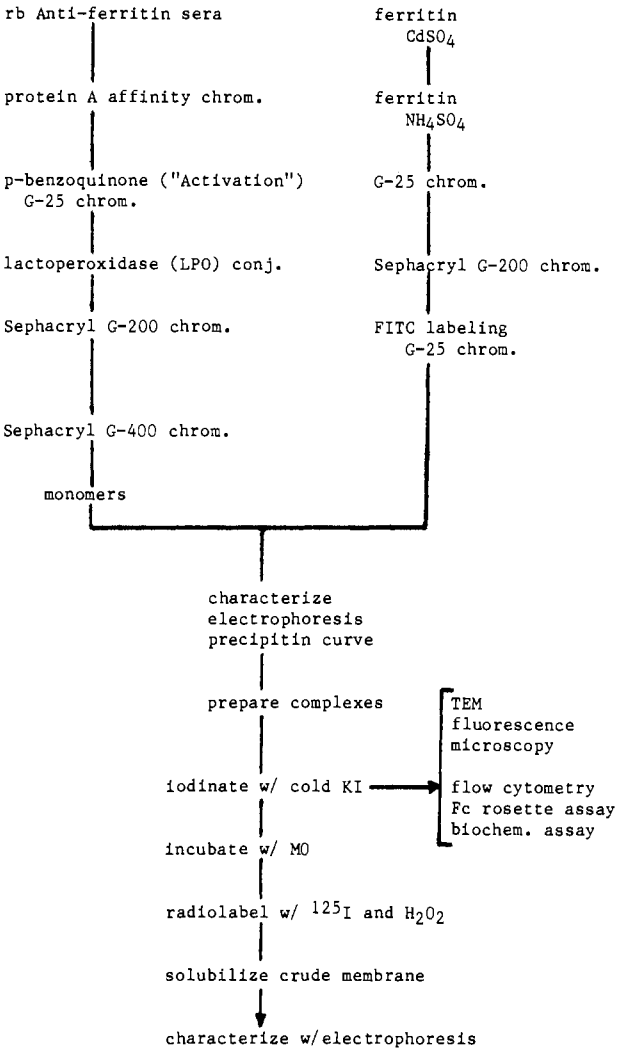

FIGURE 1: A schematic outline of the various experimental procedures. Preparation of antibody and antigen begins at upper left and right, respectively. Salt precipitation was optional, depending upon commercial suppliers.

in carbonate–bicarbonate buffer at pH 9.0 as described (Hudson & Hay, 1980). Free FITC was removed by G-25 column chromatography.

Immune Precipitation. The ability of anti-ferritin antibody and the antibody–LPO conjugate to precipitate ferritin was assessed with a quantitative precipitin test. We employed a modification of existing methodology (Hudson & Hay, 1980). Briefly, 0–500 μg of ferritin (as constituent iron) was added to a constant amount of antibody (100 μL of 1.7 mg/mL) and PBS to a volume of 350 μL. An aliquot (100 μL) of rabbit complement (Cappel Laboratories; stored at −85 °C) was added to each tube. Tubes were incubated at 37 °C for 1 h and stored at 4 °C for 7–10 days. The precipitates were washed 3 times with cold PBS, followed by dissolution with SDS. Absorbances were read in a spectrophotometer. Controls using ferritin or antibody alone were also read.

Rosette Assay. The rosette assay was performed as we have previously described (Petty et al., 1980a). Briefly, sheep erythrocytes were sensitized with rabbit anti-sheep IgG (Cordis Laboratories, Miami, FL). Sensitized cells were washed 3 times before use. Rosette calibration curves were performed each day. After incubation with immune complexes, the cells were washed twice and resuspended in HBSS at 4 °C (Petty et al., 1980). Sensitized erythrocytes (5%) were added to cells at room temperature as discussed by Wong & Wilson (1975).

Rosettes are scored as macrophages binding three or more sensitized erythrocytes.

Iodination. Cells or proteins were labeled with iodine by lactoperoxidase-catalyzed iodination. In most cases, nonradioactive ("cold") KI (Spectrum Chemical Co., Redondo Beach, CA) was used to mask antibody and antigen labeling sites prior to incubation with cells. For protein labeling, antibody–LPO conjugates or immune complexes were dialyzed against PBS. Labeling was carried out in 1 mL of PBS containing 1 mCi of ^{125}I (Amersham Corp., Arlington Heights, IL) as carrier-free NaI at 4 °C. Successive 10-μL pulses of H_2O_2 (Baker) of 0.3, 1, and 9 mM were added at 10-min intervals. The samples were then chromatographed on a Sephadex G-25 column equilibrated with PBS. The labeled proteins were collected by monitoring with a Geiger counter.

Macrophages were washed 5 times with PBS by centrifugation. For labeling, either free LPO or immune complexes were added. In the case of immune complexes, cells were washed twice to remove free complexes. Cells were kept at 4 °C at all times. Approximately (5–10) × 10^6 cells were labeled with 1 mCi of ^{125}I as described (Jones, 1980; Howard et al., 1982). Cells were washed 3 times with PBS + 5.0 mM KI and twice with PBS.

Cells were lysed with extraction buffer (0.5% Nonidet P-40, 50 mM tris(hydroxymethyl)aminomethane, 50 mM NaCl, 0.02% NaN_3, 5 mM EDTA, 50 mM phenylmethanesulfonyl fluoride, 0.2 trypsin inhibitor unit/mL aprotinin, 1 μg/mL pepsatin A, pH 8.0) for 30 min on ice. Nuclei were removed by centrifugation at 7000*g* for 15 min.

Electrophoresis and Autoradiography. Samples were analyzed by one- or two-dimensional electrophoresis in SDS–polyacrylamide gels (5, 7, or 10% acrylamide) as described (O'Farrell, 1975; Jones, 1980) by using a Bio-Rad (Richmond, CA) protean system. Samples (extracts or purified reagents) were diluted with an equal volume of sample buffer before electrophoresis. For two-dimensional electrophoresis, one of three different first-dimension methods was employed. These methods were (1) nonequilibrium pH gradient electrophoresis (NEPHGE), (2) isoelectric focusing (IEF), and (3) SDS–PAGE (without 2-mercaptoethanol) in a tube gel electrophoresis stand (Bio-Rad). Methods 1 and 2 were performed as described by Jones (1980). Method 3 was performed in the following fashion. Samples were loaded onto tube gels consisting of a stacking gel and a resolving gel. The composition of these gels is identical with that of the second-dimension slab gels. Above the sample was layered an equal volume of a 1:1 dilution of sample buffer and distilled deionized water (to minimize disturbances). Following this first-dimension run, the gel tubes were removed from the glass tubes and equilibrated with 10 mL of sample buffer containing 2-mercaptoethanol. These tubes were then affixed to a second-dimension slab gel with heated agarose. The standard procedures were then followed as above (Jones, 1980; Howard et al., 1982).

For samples containing ^{125}I, the dried gels were exposed to Fuji film (RX50) in the presence of Du Pont Lightning-Plus intensification screens for 1 day to 3 weeks (one-dimensional gels) or for 1–3 months (two-dimensional gels) in film cassettes at −85 °C.

Fluorescence Microscopy. Cells were examined in a Zeiss fluorescence microscope equipped with special excitation and detection instrumentation. The device is a combination of fluorescence recovery after photobleaching and video-intensified microscopy (Petty et al., 1980b; Willingham & Pastan, 1978). A Spectra-Physics 164-09 argon ion laser tuned to 488 nm is used for fluorescein excitation. The intensity is adjusted by plasma tube current density and by neutral density filters and a beam-splitter assembly as described (Petty et al., 1980b). The beam is spatially filtered, expanded (Earling Corp., South Natick, MA), and reflected into the epifluorescence port. A light level is chosen that does not photobleach the sample. The cells are always observed unfixed. A Leitz 50× water immersion objective is employed (numerical aperature = 1.0). For these experiments, the image is reflected onto an RCA silicon-intensifier tube held in a Dage-MTI Model 65 camera. Video signals are recorded on a Panasonic NV-8050 high-resolution video recorder and displayed on an Audiotronics monitor. The photographs reported were taken from the screen with a Polaroid camera.

Electron Microscopy. Whole-mount electron microscopy was performed by depositing ferritin on Formvar-covered and carbon-coated copper specimen grids. The samples were air-dried prior to examination. Negatively stained specimens were prepared in the same fashion except that 2% tungstophosphoric acid (Polysciences Inc.) was added 1:1 to each sample prior to deposition on grids.

Cells were fixed for 1 h with 1% glutaraldehyde in 0.1 M sodium cacodylate–HCl buffer (Polysciences Inc.), pH 7.4, containing 2% sucrose. The cells were then washed 4 times in cacodylate buffer containing 4% sucrose. Postfixation was carried out with 1% OsO_4 in 0.1 M cacodylate buffer for 1 h at room temperature. The specimens were dehydrated in ethanol and embedded in Spurr's resin (1969). The samples were thin-sectioned and examined in a Philips 201 or 301 electron microscope.

RESULTS

Electron Microscopy of Ferritin. Electron micrographs of ferritin and ferritin–anti-ferritin immune complexes are shown in Figure 2. In Figure 2, panel A, is shown a whole-mount transmission electron micrograph of a ferritin preparation used in this study. Each small electron-dense particle represents one ferritin core. Two important observations should be noted: (1) the ferritin is monodisperse and (2) there is no obvious contamination. In Figure 2, panel B, we present a similar preparation stained with 2% tungstophosphoric acid. It is apparent that each core is surrounded by an unstained protein shell. The protein shells are slightly larger than the ferritin cores given in panel B. In addition, the protein shell forms a complete circle around the core, indicating that the protein subunits have not dissociated. In Figure 2, panel C, is given a transmission electron micrograph of a ferritin–anti-ferritin immune complex. The complexes were prepared at approximately 4-fold antigen excess. The clusters of ferritin are obvious. The immune complexes are fairly uniform in size although small clusters of two or three ferritin cores can occasionally be found. In general, many (~10) ferritin molecules make up each immune complex. However, this should be regarded as a lower limit since there is likely overlapping of ferritin cores in each electron micrograph.

Quantitative Precipitin Test. In Figure 3 we show equivalence curves for anti-ferritin antibody and the anti-ferritin antibody–LPO conjugate. Since the antibodies were in purified form, it was necessary to reconstitute antisera for proper immunoprecipitation. We therefore added rabbit complement back to purified antibody or antibody–LPO conjugates. We measured antigen iron precipitated vs. total input antigen. The equivalence point has been moved slightly toward antigen excess in the case of the antibody–LPO conjugate. This study demonstrates that the antibody–LPO conjugate retains the ability to recognize antigen.

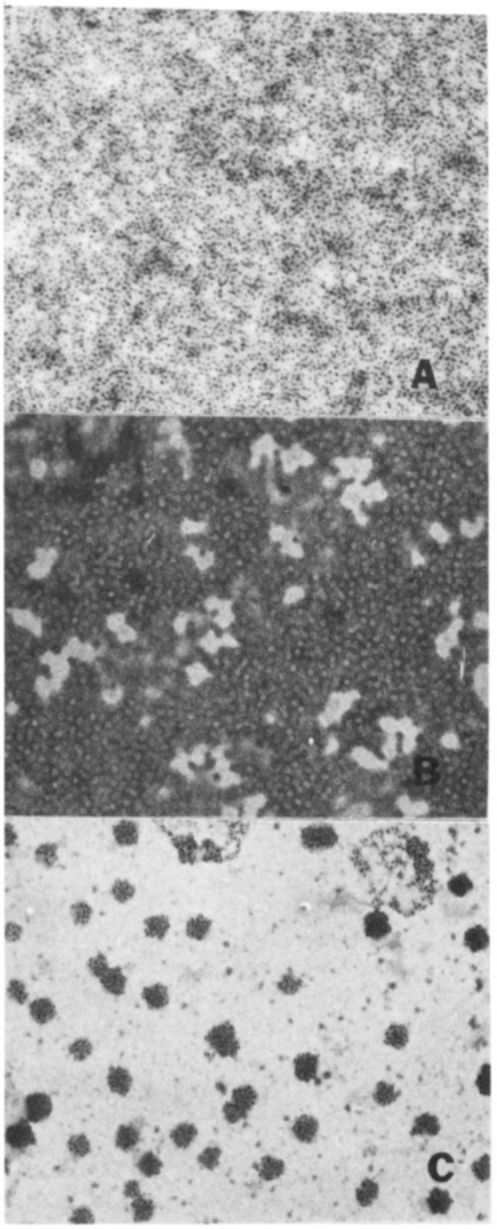

FIGURE 2: Whole-mount transmission electron micrographs of ferritin preparations. (A) Unstained ferritin showing electron-dense cores (24000×). (B) Negatively stained ferritin showing complete protein sheaths (24000×). (C) Transmission electron micrograph of ferritin–anti-ferritin–LPO immune complexes. This experiment is in roughly 4-fold antigen excess. The clusters of ferritin may be seen (12000×).

Rosette Test. Rosetting experiments measured the percent erythrocyte–antibody (EA) rosettes as a function of immune complex load. Immune complexes at 1 mg/mL in 4-fold antigen excess were added to 1 mL of RAW264 macrophages. At 0, 5, 50, and 125 μg/mL, the percent EA rosettes found were 95, 75, 23, and 12%, respectively. As the immune complex load is increased, the percent rosettes decrease in a dose-dependent manner. This demonstrates that the antibody–LPO-containing immune complexes retain the ability to block the Fc receptor.

Microscopy. Figure 4 shows a fluorescence photomicrograph of RAW264 macrophages. The silicon intensifier camera/video fluorescence system demonstrates the punctate appearance of immune complexes bound to the cell. Immune complexes were allowed to bind for 15 min on ice, followed by washing. The immune complexes bind to the macrophage cell surface in "patched" and "capped" fashion. This is consistent with earlier studies (Hess & Luscher, 1970; Pratt et al., 1979) and should be expected on the basis of the relative position on the precipitin curve; i.e., we are not in large antigen excess.

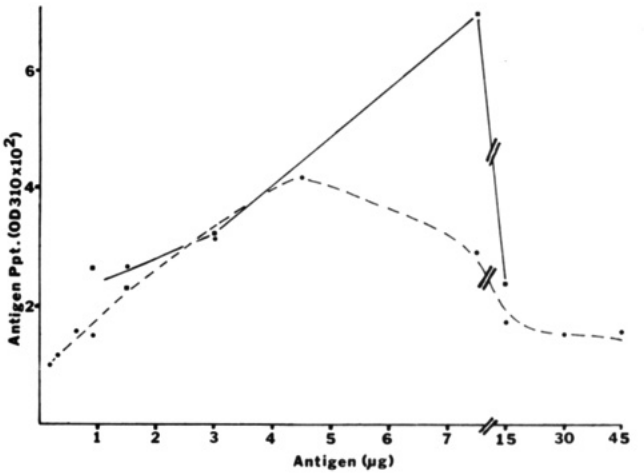

FIGURE 3: A reconstituted quantitative precipitin test of antibody and antibody–LPO conjugate immunoprecipitation. Antigen excess is to the right; antibody excess is to the left. The abscissa is total micrograms of ferritin (as constituent iron) added. The ordinate is the amount of antigen precipitated, expressed as OD 310 (iron) of solubilized precipitate. Antibody is at 1 mg/mL (– –); conjugate is at 4.78 mg/mL (—).

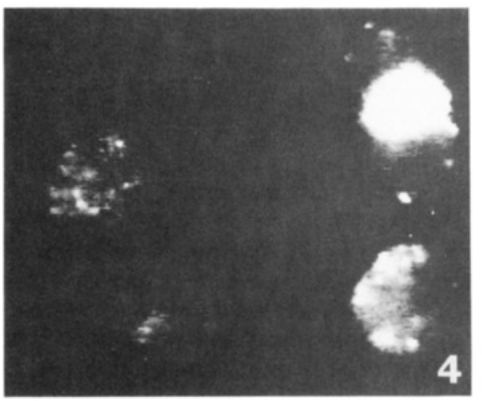

FIGURE 4: A typical fluorescence microscopic study of immune complex receptors. The cells are viewed by using silicon intensifier camera/video fluorescence microscopy. The immune complexes clearly exist as clusters in association with macrophages. The cells in the upper right show a large capped region between two cells (375×).

Thin-section transmission electron microscopy shows the clusters of ferritin bound to the cell surface. Macrophages were labeled in excess immune complexes corresponding to approximately 7% rosettes at a 1:5000 dilution of anti-erythrocyte antibody. Cells were washed to remove unbound ligand. This was followed by fixation as described above. In Figure 5 cells and complexes were cooled and then mixed together. Regions containing immune complexes are obvious. No detectable endocytosis has taken place. If cells are allowed to warm, endocytosis can be observed (data not shown), indicating that the physiological activity of stimulating endocytosis is retained by these immune complexes. The fluorescence and electron microscopic studies show that the immune complexes are delivered to the cell surface as local patches or caps, an observation that is required for the interpretation of our ^{125}I-labeling experiments (see below).

Electrophoresis. We have verified the purity and composition of antibody, LPO, and antibody–LPO conjugates with

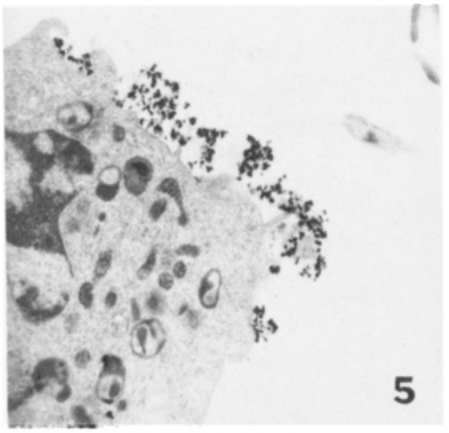

FIGURE 5: A representative survey transmission electron micrograph of immune complexes bound to RAW264 macrophages. Clusters of immune complexes can be seen (3375×).

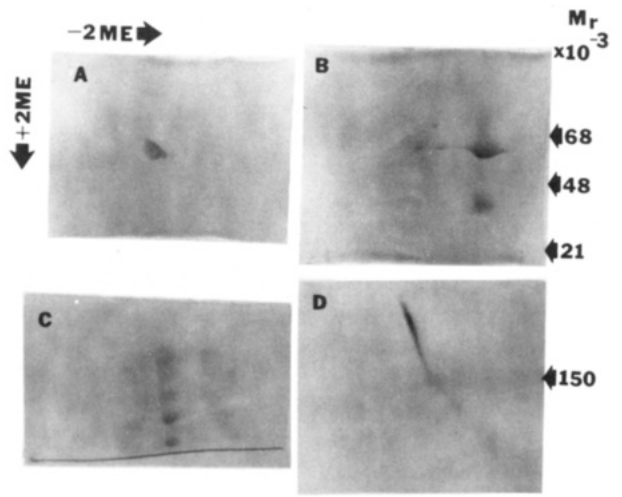

FIGURE 6: Two-dimensional SDS–PAGE experiments in the presence and absence of 2-mercaptoethanol. (A) 10% polyacrylamide gel of LPO stained with Coomassie Blue. (B) 10% polyacrylamide gel of anti-ferritin antibody stained with Coomassie Blue. The heavy and light chains are seen. (C) 7% polyacrylamide gel of "activated" antibody stained with Coomassie Blue. Protein bands in multiples of M_r 25 000 can be observed. (D) 7% polyacrylamide gel of antibody–LPO conjugate labeled with ^{125}I. Following autoradiography the band is most intense at approximately M_r 230 000.

SDS–PAGE. Protein A affinity chromatography purified rabbit anti-horse ferritin antibody gave a single band of M_r 150 000 after SDS–PAGE. Similarly, LPO yielded a homogeneous band of M_r 80 000. Two protein-containing peaks were obtained from Sephacryl S-200 column chromatography of the conjugate reaction mixture. The first peak was primarily composed of high molecular weight material (M_r >200 000; see below for further characterization). Trace amounts of free antibody can be observed; free antibody can be removed by the Sephacryl S-400 step (Figure 1). The second peak contained free LPO.

Figure 6 shows a series of two-dimensional SDS–PAGE experiments. Both dimensions are molecular weight separations. However, the second dimension contained the reducing agent 2-mercaptoethanol. Panel A shows a Coomassie Blue stained gel profile of LPO (10% polyacrylamide). No subunit composition can be discerned. As expected, antibody molecules are more heterogeneous. In Figure 6, panel B, is given a similar two-dimensional experiment of anti-ferritin antibody (also 10% polyacrylamide). Two major bands at M_r 25 000 and 50 000 can be resolved. These correspond to the light and

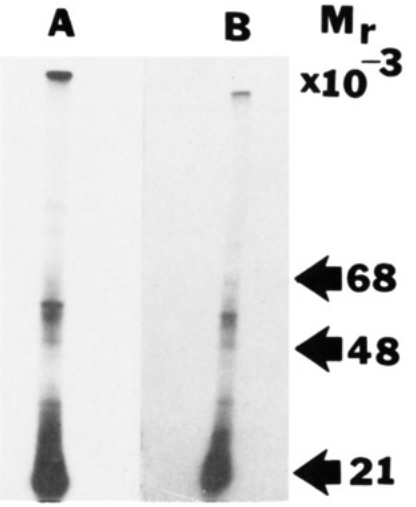

FIGURE 7: SDS–PAGE experiment of ^{125}I-labeled U937 macrophage membrane proteins using 10% polyacrylamide. (A) Membrane protein pattern obtained by using free LPO. (B) A similar experiment utilizing immune complex delivery to the cell surface. The patterns have no significant differences.

heavy chains of antibody, respectively. Some minor components of unknown origin near the molecular weight of the heavy chain can be observed in this two-dimensional gel. The effect of *p*-benzoquinone on antibody structure, in the absence of any other structure or reaction, should also be examined. The experiment was performed as described above except that, after the first stage of antibody activation with *p*-benzoquinone, lysine was added and the pH was adjusted to 9.0. The reaction product was dialyzed against PBS. The subunit structure of activated antibody is given in panel C. This is a 7% acrylamide two-dimensional gel run in the presence and absence of 2-mercaptoethanol. Five bands at approximate M_r 25 000, 50 000, 75 000, 100 000, and 125 000 can be discerned. The M_r 25 000 and 50 000 bands likely represent the light and heavy chains of antibody, as discussed above. The higher molecular weight bands from M_r 75 000–125 000 represent covalently linked combinations (via *p*-benzoquinone) of heavy and light chains (e.g., 75 000 = one heavy + one light). This indicates that interchain 2-mercaptoethanol-resistant links form during the procedure.

In Figure 6, panel D, we show a two-dimensional SDS–PAGE (with and without 2-mercaptoethanol) using 7% acrylamide. This gel shows the purified antibody–LPO conjugate. The conjugate was iodinated by using the LPO activity. A broad band is found after autoradiography. The most intense area corresponds to an M_r of 230 000–240 000. This is approximately the expected value for the heterodimer since antibody is M_r 150 000 and LPO is M_r 80 000. The heterogeneity could be a manifestation of inherent heterogeneity of starting materials and/or the loss of light chain. The ability of heavy and light chains to covalently link was demonstrated above. The results do not allow for a distinction between a linkage between the LPO and the heavy and/or light chain. However, the presence of a heterodimer is strongly indicated by the approximate molecular weight.

The antibody–LPO conjugate is capable of membrane iodination. This is shown in Figure 7. In lane A of Figure 7 is shown an autoradiograph of U937 macrophage cell surface proteins labeled with free LPO. Lane B shows a typical autoradiograph of identical cells labeled with LPO delivered by immune complexes. Cell labeling is always conducted at 4 °C to inhibit pinocytosis. To avoid unwanted proteolytic digestion during extraction, an extraction buffer containing

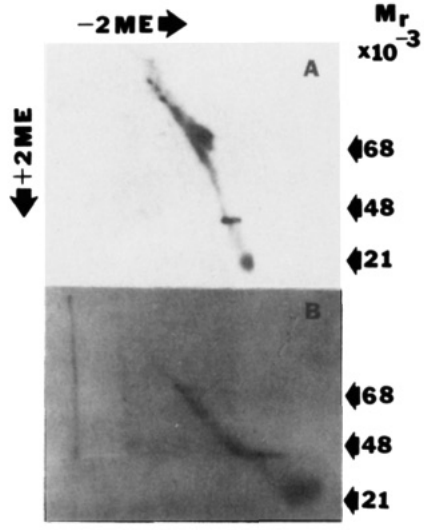

FIGURE 8: SDS–PAGE experiment of ^{125}I-labeled membrane proteins using a two-dimensional technique with and without 2-mercaptoethanol. (A) Macrophage membranes labeled with free LPO under standard conditions. (B) Macrophages labeled with local delivery of LPO by using masked immune complexes in the presence of BSA (see text for details).

a "cocktail" of protease inhibitors is required (see Materials and Methods). Experimentation revealed that improved results could be obtained with immune complexes prelabeled with nonradioactive KI. In the absence of prelabeling with cold KI, unnecessary complications of the gel profile resulted. As can be seen in comparing the profiles in lanes A and B, the labeled proteins are essentially identical. This experiment was conducted under saturation conditions, in regard to both bound immune complexes and the substrates H_2O_2 and ^{125}I. Under these experimental conditions oxidized iodine should be made available to most cell surface proteins. This is consistent with the results obtained.

We have also performed experiments under conditions of severe substrate deficit. Cell-associated ^{125}I decreases to roughly 10% of that found by using the conditions given in the preceding paragraph. In Figure 8 we show two-dimensional SDS–PAGE (with and without 2-mercaptoethanol) using free LPO (panel A) and antibody–LPO immune complexes in substrate deficit (one pulse of 0.3 mM H_2O_2) (panel B). The first experiment had conditions similar to those of Figure 7, lane A. The second study employed immune complexes bound to macrophages (cells and complexes were mixed and cooled simultaneously). Similar results are obtained at room temperature when cytochalasin B at 2×10^{-5} M is added to inhibit antibody-dependent endocytosis. Labeling was performed at 4 °C. In addition, we included 1.0 mg/mL BSA in the labeling mixture prior to addition of ^{125}I and H_2O_2. This scavenger protein would be expected to decrease the effective diffusion radius of the activated iodine molecule. ^{125}I-Labeled BSA is discarded by washing with buffer prior to extraction. A principle difference between these experiments is that upon addition of 2-mercaptoethanol a polymeric material of panel B dissociates into a broad spectrum of molecular weights. This local LPO labeling procedure suggests that an at least partially 2-mercaptoethanol-sensitive oligomerization or polymerization reaction occurs in the vicinity of immune complexes during receptor binding.

Discussion

The macrophage cell surface plays a wide variety of physiological roles [for a review, see Zuckerman & Douglas (1979b)]. One important macrophage function is the recognition of immune complexes. The study of macrophage–immune complex interaction has taken several forms. Electron microscopy (Papadimitriou, 1973; McKeever et al., 1976) and fluorescence microscopy (Hess & Luscher, 1970; Pratt et al., 1979) studies of the interaction have been reported. Flow cytometry studies have recently been presented (Titus et al., 1981). Many experiments rely on the measurement of the binding and/or degradation of radiolabeled immune complexes [e.g., Knutson et al. (1979), Finbloom (1982), and Leslie & Alexander (1980)]. Techniques for the in situ radiolabeling of cell proteins involved in immune complex recognition and processing have heretofore not been presented. This report describes our technique, which can be applied to all of the above problems, most of which can be studied simultaneously.

Under Results we discuss the preparation, characterization, and utilization of the fluorescein- and lactoperoxidase-conjugated ferritin–anti-ferritin immune complex. Several judicious choices were made in the development of this ligand. To provide a fresh approach for the study of antibody-dependent recognition, we desired a combination of biochemical and morphological approaches. Lactoperoxidase-catalyzed iodination is a widely employed method to label cell surface components (Marchalonis et al., 1971; Jones, 1980). Lactoperoxidase possesses the advantages that (i) it has substantial activity over a wide pH range (Thorell & Larson, 1978) and (ii) it can be coupled to antibody molecules with little effect on antigen-binding capacity or lactoperoxidase activity (Ternynck & Avrameas, 1976). The reagent *p*-benzoquinone was chosen for similar reasons. Ferritin has been used as an electron-dense marker in electron microscopy for many years [e.g., An et al. (1972) and Maylie-Pfenningr & Jamieson (1979)]. It has also been used as an antigen in immunological studies [e.g., Sonoda et al. (1973)]. We have additionally modified this approach by introducing a fluorescent tag on the ferritin for studies involving fluorescence microscopy or fluorescence flow cytometry. The extent of antigen modification is likely minimal. Since each apoferritin possesses 195 lysine residues (Harrison et al., 1962), only a few percent become conjugated to fluorescein isothiocyanate. Moreover, fluorescein conjugation to antibody was ruled out due to possible inhibition of Fc-domain functional characteristics (Thrasher et al., 1975).

Whole-mount and negative-stain transmission electron microscopy has demonstrated that the ferritin we have utilized is monomeric, intact, and uncontaminated. Since oligomers contain more antigenic sites per molecule, this would affect the nature of the complexes. Electron microscopic studies on horse ferritin oligomers (Williams & Harrison, 1968) and ferritin assembly (Pape et al., 1968) have been reported. Our interpretations are in agreement with those of previous investigators. Moreover, our studies of ferritin–anti-ferritin complexes are in agreement with previous reports [e.g., Feinstein & Rowe (1965)].

The chemical nature of conjugated protein ligands should be examined to provide structural information. Our studies indicate that the LPO-conjugated antibody we have employed is a heterodimer of 230000 daltons. The conditions described above favor heterodimer formation. Activation of antibody required only 30 min. Longer incubations produced insoluble aggregates. The high LPO-to-antibody ratio is an improvement over earlier techniques. During the second step of the conjugation, the probability of antibody-to-LPO binding was thereby increased. The approach markedly enhanced the yield of heterodimers. In our hands we found predominantly higher

order oligomers with the earlier method (data not shown).

Chemically modified ligands must be shown to retain functional activity if physiological relevance is to be inferred. Two important criteria have established that antibody–LPO conjugates retain functional capacities. Since the conjugates were purified by column chromatography, free antibody or LPO could not account for these functional properties. First, conjugates retain antigen-binding activity as demonstrated by precipitin analysis. Since antibody was purified initially, it was necessary to reconstitute the precipitin assay with normal rabbit complement. In the absence of complement, complexes remain essentially soluble and precipitation cannot be reliably measured. In the presence of rabbit complement the immune reaction is quickly obvious. Controls involving the absence of antibody, antigen, and complement or the presence of heat-inactivated complement were routinely performed. Two important observations can be gleaned from this experiment. The antibody–antigen reaction was occurring. Therefore, the Fab region must retain considerable activity after conjugation. Moreover, since complement-binding activity is usually ascribed to the CH3 homology of the Fc domain of IgG antibody, then much functional ability must be retained here also. In the second type of functional study, we demonstrated that antibody–LPO conjugates in immune complexes retain the ability to block Fc receptors of RAW264 macrophages in a dose-dependent fashion. We have shown this by using a rosette assay.

The LPO incorporated into the immune complexes retains the ability to iodinate cell surface proteins. This was shown by using ^{125}I and H_2O_2, followed by SDS–PAGE and autoradiography. It is important to recall that free LPO was removed by column chromatography and verified by SDS–PAGE. The exhaustive iodination procedure we have used is roughly equivalent to the free LPO labeling protocol. The membrane protein autoradiograph obtained is essentially identical with that found with free LPO. This suggests that the membrane was not perturbed in any substantial fashion (e.g., lysed). If locally delivered LPO is allowed to generate considerable reaction product, indiscriminant membrane protein labeling is obtained. This was the anticipated result since a large amount of I^+ would be expected to label the membrane in a global fashion. The presence of antibody–antigen ligand did not influence the membrane protein pattern. This "masking" effect was due to prelabeling ligand with nonradioactive iodine. This important variation on earlier methods deconvolutes the interpretations. It may be applicable to many other ligand–receptor studies.

The local LPO delivery protocol was then employed to label cell surfaces under conditions of substrate deficit. Small amounts of I^+ will be generated. As described above, the masked immune complexes cannot be self-iodinated. Cell surface membrane proteins are the expected target of the I^+. When small quantities of I^+ are available, sites near the immune complexes should be preferentially labeled. Moreover, BSA was included in the labeling protocol to scavenge free I^+, which may diffuse from the area of immune recognition. Both of these strategies improve the selective labeling of proteins near the immune complex. This experiment revealed that an oligomerization or polymerization of proteins occurs at the cell surface during immune complex recognition. This reaction is at least partially sensitive to the reagent 2-mercaptoethanol.

The polymerization product was observed as a "streak" in the +2-mercaptoethanol dimension, with little resolution of distinct proteins. This effect may be due to incomplete reduction of proteins. Alternatively, oxidative metabolites released upon immune complex binding could catalyze additional cross-linking reactions of surface proteins independent of the sulfhydryl oxidation previously described (Jasin, 1983; Stahmann et al., 1977). If such reactions were occurring randomly, a collection of protein products of ill-defined molecular weight would be expected. After reduction with 2-mercaptoethanol the polymeric material has molecular weights equal to or greater than 40 000. Since no smaller proteins are found as part of the polymer, it is consistent with the idea that additional biochemical mechanisms may be linking smaller proteins together or to larger proteins.

The polymerization step may be driven by oxidative products released from phagocytes (Petty et al., 1985). Also consistent with this observation is that membrane-impermeable sulfhydryl-blocking reagents inhibit phagocytosis (Dereski & Petty, 1985). These observations support the sulfhydryl-redox model of antibody-dependent phagocytosis (Petty, 1985). This hypothesis states that membrane protein sulfhydryl groups undergo oxidation in the course of endocytic triggering.

There are numerous possible applications of this immune complex ligand in the studies of immune recognition and immune complex mediated diseases. The immune complexes we have described are particularly versatile. They should be amenable to separate or simultaneous analysis by (1) fluorescence microscopy, (2) electron microscopy, (3) microscopic autoradiography, (4) fluorescence-activated cell sorting, and (5) lactoperoxidase-catalyzed iodination of the plasma membrane and/or intracellular compartments. Moreover, radiolabeled immune complex could be employed to follow degradation. Immune complex receptors on many other cell types could also be examined. In addition, this approach may be applicable to many other types of ligand–receptor interaction.

References

An, T., Miyai, K., & Sell, S. (1972) *J. Immunol. 108*, 1271.

Bourguignon, L. Y. W. (1979) *J. Cell Biol. 83*, 649.

Dereski, W., & Petty, H. R. (1985) *Immunology 54*, 397.

Feinstein, A., & Rowe, A. J. (1965) *Nature (London) 205*, 147.

Finbloom, D. S. (1982) *Cell. Immunol. 74*, 305.

Hess, M. W., & Luscher, E. F. (1970) *Exp. Cell Res. 59*, 193.

Howard, F. D., Petty, H. R., & McConnell, H. M. (1982) *J. Cell Biol. 92*, 283.

Hudson, L., & Hay, F. C. (1980) *Practical Immunology*, Blackwell, London.

Jasin, H. E. (1983) *J. Immunol. 130*, 1918.

Jones, P. P. (1980) *Selected Methods in Cellular Immunology* (Mishell, B. B., & Shiigi, S. M., Eds.) p 398, W. H. Freeman, San Francisco.

Knutson, D. W., Kijlstra, A., & van Es, L. A. (1979) *J. Immunol. 124*, 2040.

Lauber, K. (1965) *Z. Klin. Chem. 3*, 96.

Leslie, R. G. Q., & Alexander, M. D. (1980) *Curr. Top. Microbiol. Immunol. 88*, 25.

Lowry, O. H., Rosebrough, N. J., Farr, A. L., & Randall, R. J. (1951) *J. Biol. Chem. 193*, 265.

Marchalonis, J. J., Cone, R. E., & Santer, V. (1971) *Biochem. J. 124*, 921.

Maylie-Pfenninger, M. F., & Jamieson, J. P. (1979) *J. Cell Biol. 80*, 69.

McKeever, P. E., Garvin, A. J., Hardin, D. H., & Spicer, S. S. (1976) *Am. J. Pathol. 84*, 437.

Mellman, I. S., & Unkeless, J. C. (1980) *J. Exp. Med. 152*, 1048.

Papadimitriov, J. M. (1973) *J. Pathol. 110*, 213.
Petty, H. R. (1985) *Mol. Immunol.* (in press).
Petty, H. R., Hafeman, D. G., & McConnell, H. M. (1980a) *J. Immunol. 125*, 2391.
Petty, H. R., Smith, L. M., Fearon, D. T., & McConnell, H. M. (1980b) *Proc. Natl. Acad. Sci. U.S.A. 77*, 6587.
Petty, H. R., Dereski, W., Francis, J., Fox, B., & Boxer, L. A. (1985) *Clin. Res.* (in press).
Pratt, D. S., Katilus, J., Dreisin, R. B., Robinson, H. M., & Schwarz, M. I. (1979) *J. Immunol. Methods 27*, 127.
Raschke, W. C., Baird, S., Ralph, P., & Nakoinz, I. (1978) *Cell (Cambridge, Mass.) 15*, 261.
Rifkind, R. A., Hsu, K. C., & Morgan, C. (1964) *J. Histochem. Cytochem. 12*, 131.
Sonada, S., Shigematsu, T., & Schlamowitz, M. (1973) *J. Immunol. 110*, 1682.
Spurr, A. R. (1969) *J. Ultrastruct. Res. 26*, 31.
Stahmann, M. A., Spencer, A. K., & Honold, G. R. (1977) *Biopolymers 16*, 1307.
Sundstrom, C., & Nilsson, K. (1976) *Int. J. Cancer 17*, 565.
Ternynck, T., & Avrameas, S. (1976) *Ann. Immunol. (Paris) 127C*, 197.
Thorell, J. I., & Larson, S. M. (1978) *Radioimmunoassay and Related Techniques*, Chapter 3, Mosby, St. Louis, MO.
Thrasher, S. G., Bigazzi, P. E., Yoshida, T., & Cohens, S. (1975) *J. Immunol. 114*, 762.
Titus, J. A., Sharrow, S. O., Connolly, J. M., & Segal, D. M. (1981) *Proc. Natl. Acad. Sci. U.S.A. 78*, 519.
Willingham, M. C., & Pastan, I. (1978) *Cell (Cambridge, Mass.) 13*, 501.
Wong, L., & Wilson, J. D. (1975) *J. Immunol. Methods 7*, 69.
Young, J. D. E., Unkeless, J. C., Kaback, H. R., & Cohn, Z. A. (1983a) *Proc. Natl. Acad. Sci. U.S.A. 80*, 1636.
Young, J. D. E., Unkeless, J. C., Kaback, H. R., & Cohn, Z. A. (1983b) *Proc. Natl. Acad. Sci. U.S.A. 80*, 1357.
Zuckerman, S. H., & Douglas, S. D. (1979a) *CRC Crit. Rev. Microbiol. 7*, 1.
Zuckerman, S. H., & Douglas, S. D. (1979b) *Annu. Rev. Microbiol. 33*, 267.

Formaldehyde Metabolism by *Escherichia coli*. Carbon and Solvent Deuterium Incorporation into Glycerol, 1,2-Propanediol, and 1,3-Propanediol†

Brian K. Hunter
Department of Chemistry, Queen's University, Kingston, Ontario, Canada
Kathryn M. Nicholls and Jeremy K. M. Sanders*
University Chemical Laboratory, Lensfield Road, Cambridge CB2 1EW, United Kingdom
Received November 15, 1984

ABSTRACT: *Escherichia coli* were grown on 14.3% uniformly ^{13}C-labeled glucose as the sole carbon source and challenged anaerobically with 90% ^{13}C-labeled formaldehyde. The major multiply labeled metabolites were identified by ^{13}C NMR spectroscopy to be glycerol and 1,2-propanediol, and a minor metabolite was shown to be 1,3-propanediol. In each case, formaldehyde is incorporated only into the C_1 position. A novel form of ^{13}C NMR isotope dilution analysis of the major products reveals that all the 1,2-diol C_1 is formaldehyde derived but that about 40% of the glycerol C_1 is derived from bacterial sources. Glycerokinase converted the metabolite [1-^{13}C]glycerol to equal amounts of [3-^{13}C]glycerol 3-phosphate and [1-^{13}C]glycerol 3-phosphate, demonstrating that the metabolite is racemic. When [^{13}C]formaldehyde incubation was carried out in H_2O/D_2O mixtures, deuterium incorporation was detected by β- and γ-isotope shifts. The 1,3-diol is deuterium labeled only at C_2 and only once, while the 1,2-diol and glycerol are each labeled independently at both C_2 and C_3; C_3 is multiply labeled. Deuterium incorporation levels are different for each metabolite, indicating that the biosynthetic pathways probably diverge early.

Formaldehyde is a well-known antibacterial agent. However, we have recently shown that *Escherichia coli* can detoxify low concentrations of formaldehyde by metabolism to relatively innocuous products (Doddrell et al., 1984; Hunter et al., 1984). Using in vivo NMR[1] spectroscopy, we demonstrated the formation of formate, methanol, and three unidentified products; we now report that these unknowns are glycerol (1,2,3-propanetriol), 1,2-propanediol, and 1,3-propanediol. We present isotope labeling evidence concerning both the natural pool size of these products and the mechanism of their biosynthesis.

When *E. coli* suspensions are challenged with a 10 mM aqueous solution of ^{13}C-labeled formaldehyde, the resulting metabolism can be observed by ^{13}C NMR (Hunter et al., 1984) and by ^1H NMR (Doddrell et al., 1984). Further experiments have established that the previously described metabolism is mainly anaerobic unless air is actively bubbled through the suspension in the spectrometer (B. K. Hunter, unpublished results). The two major unidentified species give ^{13}C signals from the labeled carbon at 64 and 68 ppm; a minor species of variable intensity appears at 60 ppm. In proton-

† This work was supported by funds from the U.K. Science and Engineering Research Council (to K.M.N. and J.K.M.S.) and the Hickinbottom Bequest of the Royal Society of Chemistry (to J.K.M.S.).

[1] Abbreviations: ATP, adenosine 5'-triphosphate; d, doublet; NADH, reduced nicotinamide adenine dinucleotide; NMR, nuclear magnetic resonance; NOE, nuclear Overhauser enhancement; ppm, parts per million; s, singlet.

0006-2960/85/0424-4148$01.50/0